

Cosmic Rays, Aerosol-Photosynthesis and Vegetational Air Ion

Otto Ziep

Independent Scholar, Berlin, Germany

Email: ottoziep@gmail.com

How to cite this paper: Ziep, O. (2025) Cosmic Rays, Aerosol-Photosynthesis and Vegetational Air Ion. *Journal of Modern Physics*, **16**, 1179-1192.

<https://doi.org/10.4236/jmp.2025.168059>

Received: June 6, 2025

Accepted: August 22, 2025

Published: August 25, 2025

Copyright © 2025 by author(s) and Scientific Research Publishing Inc.

This work is licensed under the Creative Commons Attribution International License (CC BY 4.0).

<http://creativecommons.org/licenses/by/4.0/>



Open Access

Abstract

Atmospheric ionization and cloud radiative forcing are extended fractal as a cosmic-ray-charge-cloud superfluid also to biosphere. Measured air ion variations in vegetation areas are proven as an alternating flow in a chaotic circuit present in all points of atmosphere and biosphere. Within the additive model of continuous creation of matter, a quadratic model also describes organic aerosols and links photosynthesis to cosmic rays.

Keywords

Cosmic Rays, Aerosol, Photosynthesis, Vegetational Air Ion, Continuous Creation of Matter

1. Introduction

Galactic cosmic rays (GCR) and aerosols in Earth's atmosphere and their role in cloud formation are controversially discussed [1]-[3]. The hypothesis of GCR-condensation nuclei (CN)-cloud condensation nuclei (CCN) dependence in clouds (GCR-CN-CCN) includes organic species as well. As an external source, organic aerosol grows CN into the size of CCN [4]. GCR sources in the atmosphere act as both sinks and sources for aerosols [5]. Measurements have indicated that organic species may make up a significant portion of CCN and contribute significantly to the aerosols in the troposphere [4]. Despite low vacuum energy density of GCR $\rho_{vac}(\text{GCR}) \approx 1 \text{ eV} \cdot \text{cm}^{-3}$ which combines a low GCR-count rate with ultra-high GCR-energy the influence of GCR-CN-CCN on climate is discussed. $\rho_{vac}(\text{GCR})$ is comparable to $\rho_{vac}(\text{CMB}) \approx 0.26 \text{ eV} \cdot \text{cm}^{-3}$, $\rho_{vac}(\text{star}) \approx 0.3 \text{ eV} \cdot \text{cm}^{-3}$ of the microwave background (CMB). A fractal zeta universe (FZU) extends the GCR-CN-CCN hypothesis to a cosmic ray-charge-cloud-superfluid unit (CRCCS) where spacetime belongs to an iterated, complex, non-conserved, overdetermined Lagran-

gian with third derivatives in a Schwarzian derivative [6] [7]. Additive or multiplicative creation of matter also includes the origin of GCR [8]. GCR-isotropy favors a homogeneous model for every point. GCR CRCCS is a self-similar bifurcating spacetime where strong tensile forces are responsible for GCR [7]. For all points, CRCCS is an open but interconnected system of spacetime oscillations. Large massive fragments of positive charge and negative air ions are surrounded by non-radiative bifurcating spacetime trees (BST). This behavior is a peculiarity of the quadratic transformation of the Weber invariant $f(\omega)$ where $f(\omega)f(\omega') = \sqrt{2}$ [7]. A non-stationary BST-GCR-source is claimed in every universe point also on Earth. FZU is capable of including the cosmological constant problem (CCP), quantum entanglement (QE), cosmological redshift and expansion and the speed limit as realizations of simplest cycles of spacetime curvature. The present paper claims that photosynthetic reactions are bound with low count rate to BST. Ambient ions are continuously generated by galactic cosmic rays at a low rate of $\rho_{\text{GCR}} \approx 2 \text{ cm}^{-3} \cdot \text{s}^{-1}$ ion-pairs at ground level and up to $\rho_{\text{GCR}} \approx 20 - 30 \text{ cm}^{-3} \cdot \text{s}^{-1}$ ion-pairs in the upper troposphere leading to simulated CCN ion densities up to 10^4 cm^{-3} [3]. The ratio of ρ_{vac} to molecular $\rho_{\text{core}} \approx 10 \text{ g} \cdot \text{cm}^{-3}$ in the Earth's core gives a factor 10^{31} . Measured ion densities $\rho_{\text{ion}} \approx 10^5 \text{ cm}^{-3}$ in vegetational areas are 10^{10} times higher as compared to ρ_{vac} (GCR) which are a few protons in 1 m^3 . Photosynthesis is explained by excitonic reactions and photon exchange of about 1 eV with bound energy $E_{\text{exc}} = \frac{e^2}{4\pi\epsilon_0\epsilon R}$ of molecules of charge e and radius R [9].

Photosynthesis is correlated nonlocal in time over years and areas of km^2 . Solar incoming flux of about 10^2 Wm^{-2} and organic binding energy of about 10^2 kcal/mol corresponds to organic matter of 1 mol for either 10^4 h on 1 cm^2 or for 1 h on 1 m^2 . GCR area detector arrays use a relation between energy and correlation. Due to BST the present paper suggests a participation of ultra-high correlated GCR components at photosynthesis [5] [10]. In vegetation areas diurnal variation of positive and negative air ions at ground level is $\rho_{\text{ion}} = 0.294, 0.480, 7.62$ and that of positive air ions is $\rho_{\text{ion}} = 1.890, 1.380, 4.94$ in units of $10^5 \text{ ions} \cdot \text{cm}^{-3}$ for e.g., Papaya [11] [12]. CRCCS is a quadratic model for creation of matter like a zero-energy universe/cavity, as a nontrivial zero of the zeta function [13]. Mathematical BST-sources are zero-energy cavities as stable orbiting zeros of zeta functions by quadratic mass iterations. Oscillating spacetime-curvature is stable periodic orbits of elliptic invariants with unstable bifurcating k-components. FZU proves a self-similar ratio $\kappa_{\text{BO}} \approx 10^{20}$ of the order of the Avogadro constant. Self-similarity of the cloud-in-cloud mass ratio implies self-similarity $\kappa_{\text{BO}} \rightarrow \kappa_{\text{BO}}^4$ [14]. Also, ion creation experiments at Alpine waterfalls or by aerodynamic breakup create large fragments of positive charges surrounded by negative charge [15]-[17]. CRCCS created from a zero-energy state is a three-component open system with complex Lagrangian. A complex Lagrangian algorithm is described in Section 2 based on finitely generated binary elliptic invariants. A theta constant source of CRCCS is proposed in Section 3. Section 4 discusses a possible three-

component state of charges, bound states and complex dark matter. Section 5 discusses correlations in photosynthesis. Open cloud systems of ionization, nucleation and coagulation are described by an overdetermined, complex Lagrangians $L(\{F(f, z), z\}) = L(F, \dot{F}, \ddot{F}, \ddot{\ddot{F}})$ by minimizing the error caused by the Schwarzian derivative $\{F(f, z), z\}$. If iterated L contains quadratic mass terms $\delta m, \delta m'$, negative fluctuations δm are possible. A negative mass is required in the additive model of continuous creation of matter [8]. A tidal force or van der Waals force depends on a product $\delta m, \delta m'$. Section 5 uses a mathematical one-to-one relation between organic molecules and binary invariants. In Section 2, the paper claims that the increase of atmospheric GCR rates at ground level up to factor of 10^{10} from that of ρ_{vac} (free space) is caused by elliptic invariances $f \rightarrow 1/f$ and $\lambda \rightarrow 1/\lambda$. Measurements of high values of ρ_{ion} in vegetation areas indicate the validity of e.g., a $\lambda \rightarrow 1/\lambda$ transition where the Legendre module is viewed as a current density [11] [12]. A discussed amount of BST energy claimed in Section 4 is used to explain that artificial photosynthesis is currently difficult to control. A possible use of ultra-high energy excitations at quantum Hall effect (QH) and in biopower plants has been predicted [14]. Aerial biomass can be modeled by a 6-parametric Lotka-Volterra (LV) model, which justifies a quadratic map [18]. The logistic model is contained in the 5-4 parametric quadratic map $F(f, z)$ used in the present paper.

2. Complex Dark Matter and Elliptic Symmetries

Spacetime and physical fields result from a minimum of a real Lagrangian L . Complex structures yield an overdetermined functional L where nonstationary states are plausible by error minimizing least squares. A complex structure is dark matter above a detection limit. A complex differentiable state requires a holomorphic function. The holomorphic Riemann ξ -function is fractionally substituted at its zeros z_{nt} which serves as a definition of rational values. Chaotic maps depend weakly on the starting point. Subsequent rational quadratic maps tend to binary Weber invariants $f(\omega)$ and create a complex multiplication endomorphism for periods ω [19]. Iterated units $l = \ln f(\omega)$ become circulating due to the theorem of Sharkovskii. An optimal regulator index $R_\Delta = \det l$ enters the complex conformal Lagrangian as a minimum of a quadratic form in l with auxiliary Lagrange conditions. Determinantal complexity of R_Δ reduces approximately to a simple trace of the matrix exponential of the Lagrangian L . In a first approximation R_Δ is a circulant closed contour integral $\exp \oint d\nu L = \exp \oint d\nu l$. Cyclic l in L are expected as roots of unity on the second exponentiation level. This corresponds to an additive term in L given by the Euclidean norm which is equivalent to a quartic Bezout matrix B_4 within the algorithm in **Figure 1**. A singular B_4 results in a holomorphic B_8 whose frequencies are relevant for physical fields. Starting from the unit $1 = e^{\xi(z_{nt})} = \prod_n e^{n^{-z_{nt}}}$ the entire polynomial $\xi(z)$ contains all frequencies. The iterated $\xi(z)$ -function is then a clock frequency $z_k = \xi(z) = \partial\varphi/\partial z \approx (\varphi(z) - \varphi(w))/(z - w)$ of an algorithm for the

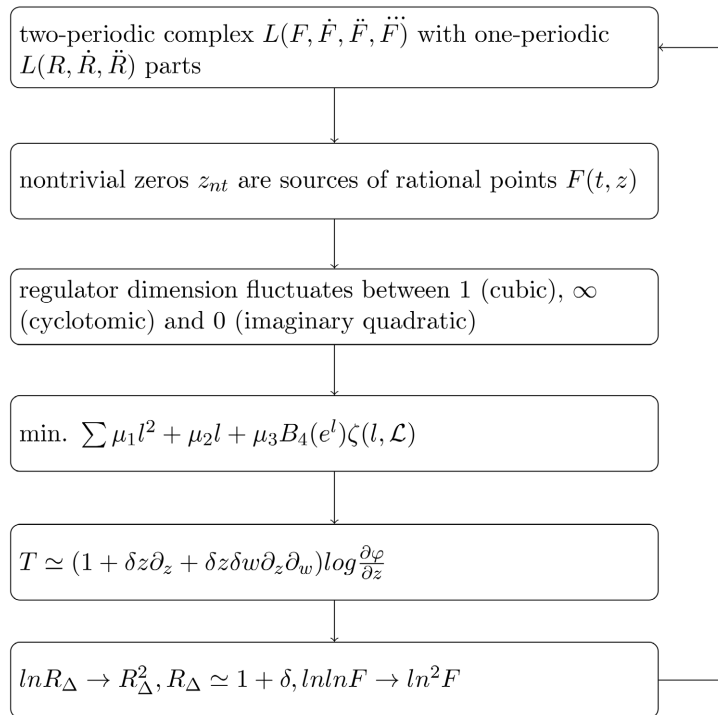


Figure 1. Schematic algorithm for a complex, unified Lagrangian $L(F, \dot{F}, \ddot{F}, \ddot{\ddot{F}})$.

optimal regulator R_Δ in **Figure 1** for $l = \ln z_k$.

$$R_\Delta \approx \exp \oint d\nu l \approx \exp \oint d\nu L \approx 1$$

$$\oint d\nu L = \sum_{z_{nt}} \oint d\nu \ln(z - z_{nt}) \Big|_{z=\lambda} \approx 2\pi k$$

which is invariant with respect to symbolic linear transformations $\gamma(\phi_3)$ of cubic invariants. The Schwarzian derivative $\{\varphi(z), z\}$

$$\partial_z \partial_w \log \frac{\partial \varphi}{\partial z} = \{\varphi, z\} = \frac{\ddot{\varphi}}{\dot{\varphi}} - \frac{3}{2} \left(\frac{\ddot{\varphi}}{\dot{\varphi}} \right)^2$$

is a negative for a non-symbolic quadratic map of cubic roots in $\gamma(\phi_3(f(\omega))) \circ z$ which is a criterium of a chaotic map. For subsequent regular, chaotic steps $\xi(\xi \dots \xi)$ and $\varphi(\varphi(\dots \varphi))$ one gets a scale factor $R(t)$

$$\dot{\varphi} = \prod_k \dot{\varphi}_k = R(t) \rightarrow \exp(\lambda_L) \rightarrow \exp(\lambda_L 2^k).$$

A slowly varying Lyapunov exponent λ_L constitutes the Ricci scalar $\frac{\ddot{R}}{R} + \left(\frac{\dot{R}}{R}\right)^2$ with scale factor $R(t)$. An extra term $\frac{-5}{2} \left(\frac{\dot{R}}{R}\right)^2$ describes possibly matter if trajectories vary slowly [20]. Complex conformal non-stationary processes are reducible to stationary processes inherent to real spacetime for a real Lagrangian. Functions $F(t, z)$ are equivalent to the inverse fermion Green's function G^{-1} . Mean fields are $\partial F(t, z)$ that enter the following algorithm [20].

Simplest cycles yield are equivalent to an addition theorem where the Euclidean

norm $N(E_q)$ of four states equals a Bezout matrix $B_4(E)$. A singular $B_4(E)$ corresponds to a non-singular $B_8(E)$ of order eight, which corresponds to a holomorphic four-component complex quadruple for elliptic addition with units E . Terms proportional to μ_2 and μ_3 in **Figure 1** are viewed as ionization rates, which is plausible because the geometric zeta function $\zeta(l, \mathcal{L})$ is Bose-like, which is kept constant here. The paper claims that atmospheric ionization, cloud radiative forcing, and biospheric photosynthesis are linked through CRCCS by a conformal complex Lagrangian. Within this view, the dark, highly correlated, non-radiative, non-dissipative state should also concern the biosphere. Moreover, the quadratic transformation $\omega \rightarrow \omega'$ obeys symmetries $f(\omega)f(\omega') = \sqrt{2}$ with involution $i^2(\lambda) = 1$ where $\lambda \rightarrow i(\lambda) = 1 - \lambda, 1/\lambda$. The paper claims that the BST flux increases again on ground level as a result of involution $\lambda \rightarrow i(\lambda)$. Physical fields mean one-periodic states. Oscillations in a negative differential branch of a chaotic quadratic map $\gamma(\phi_3(f(\omega)))$ for a cubic $\lambda i(\lambda) = 2^4/f^{24}(\omega)$ are related to a mass term $\delta m \cdot \delta m' = 0$. The involution $\lambda \rightarrow 1/\lambda$ is set in context to the geosphere and atmosphere. FZU claims that periods ν_{sh} due to the theorem of Sharkovskii are supplemented by pseudo-congruent and finitely generated binary invariants $f(\omega)$ on a contour $d\nu$ in w -dimensional complex space. Regarding $\varphi(z)$ as a current and $\xi(z)$ as an electric one-dimensional field subsequent maps $\gamma \circ \dots \circ \gamma$ allow to introduce a dimensionless coupling constant G_w . Taking $\lambda = \xi^{-1} = z$ in (2) as a current j_m described by a bispinor ψ one gets similarities for all interactions $w = 1, 2, 3, 4, 5$ (strong, weak, electromagnetic, gravitation, dark).

$$T \approx \rho_{vac} \approx \sum_i G_w E_i^2 \approx \gamma \circ \dots \circ \gamma \circ \lambda \quad (1)$$

Physical quantities appear for regulator indices $R_\Delta = 1$ close to 1 with $\lambda = 1$ or $\lambda = 0$. Stress-energy T enters the flowchart where one-periodic units are $E_i \approx \varepsilon_{p-1}^i \varepsilon_p^{8^{p-i}}$ with generators ε_{p-1} and ε_p . A cubic $\phi_3(E) = 0$ should imply $\varepsilon_p = e^{G_w \phi_3(E)}$. An interaction concerns dimensionless fields where ratios G_w/G_{w-1} are supported by experimental data. The coupling constant $G_w = \gamma \circ \dots \circ \gamma$ reflects fixed points of a quadratic map $\gamma(\phi_3(f(\omega)))$ of elliptic Weber invariant $f(\omega)$ for imaginary terms in $\oint d\nu l$. The 4-5-parametric γ -map is a Hermite-Tschirnhausen substitution of cubic polynomial ϕ_3 with 4 parameters as a projection of a quartic polynomial with 5 parameters [14]. A sum over discrete second derivatives $z_k - 2z_{k+1} - z_k$ in the Schwarzian derivative $\partial_z \partial_w \log \frac{\partial \varphi}{\partial z}$ yields nested $\frac{1}{3}$ segments in a Cantor set. A Cantor set yields the coupling constant $\ln G_w = -w! 2^w \ln_3^w 2$ which agrees with the order of magnitude of ratios of G_w in experiment. If this value of the exponent is viewed as an approximation of $\log^w(1+y)$ with dropping all powers of y^{p-1} one approximates for $p=11$ coupling constants by cyclotomic Jacobi-Gauss-Lagrange periods as a power

tower in w [20] [21]. Zeros $z_{nt} \simeq \lambda$ imply a sequence of rational iterated values $\gamma \circ \xi$. The claim is that stress-energy T in (1) is iterated λ within a four-component representation including $i(\lambda)$

$$\lambda = \frac{1}{2} + \frac{j_m}{m} \tag{2}$$

which can be mapped to a Dirac current $j_m = \bar{\psi} \lambda_m \psi$ on a strip $z_{nt} = \frac{1}{2} \pm im_n$ of nontrivial zeros of $\xi(z)$. Fluctuating λ are currents in CRCCS due to elliptic curves E_λ . Iteration steps $\gamma(\phi_3(f(\sqrt{\Delta})))$ with $\lambda i(\lambda) = 2^4 / f^{24}(\omega)$ change periods ω . Equivalent periods $\begin{pmatrix} 1 & 0 \\ 0 & 1 \end{pmatrix} \omega$, $\begin{pmatrix} 0 & -1 \\ 1 & 0 \end{pmatrix} \omega$ or quadratic transformed periods $\begin{pmatrix} 1 & -1 \\ 1 & 1 \end{pmatrix}$ obey invariances

$$(1 - \lambda i(\lambda))^3 / (\lambda i(\lambda))^2 = const, f(\omega') = \sqrt{2} / f(\omega) \tag{3}$$

yielding $\lambda \rightarrow i(\lambda), 1/\lambda, 1/i(\lambda), 1-1/\lambda, -\lambda/i(\lambda)$. It is conjectured that this involution correlates low and high values of the energy density inherent in each spacetime point. It is claimed that the hexagonal symmetry of λ_k due to the invariance (3) changes into a spherical symmetry. Interchanging two points $2 \rightarrow 3$ in two pairs 1, 2 and 3, 4 one gets $\lambda \rightarrow 1/\lambda$ and $j_m \rightarrow 1/j_m$ on opposite sides of the sphere: A high-speed limit in the inner sphere turns out a low-speed limit in the outer sphere. Accordingly, it is claimed that in elliptic symmetry a GCR air shower with velocity of light has its counterpart within slow plant growth. Moreover, symmetries $\lambda_k \rightarrow 0$ and $i(\lambda_k) \rightarrow 1$ in Equation (3) would interchange ground level and upper atmospheric levels changing energy densities from the vacuum ρ_{vac} to the core ρ_{core} . At each step λ_k the elliptic invariant (3) would be capable of describing large fragments surrounded by light atmospheric components. Elliptic field equations emerged in Friedmann solutions [22]. Fluctuations on elliptic curves on toroidal and hyperelliptic bifurcating lattices are claimed for all interactions within FZU. Real spacetime results from an one-dimensional stationary process of complex bifurcating curvature. This stationarity is suspected in an underlying pseudo-congruence in k-components. The pseudo-congruent correlation is claimed as QE [23]. The present paper transmits this stationary correlation also to photosynthesis. A $\lambda \rightarrow 1/\lambda$ transition would be capable to correlate low with high values of the energy density within the CCP [14].

3. A Theta Constant Source

Invariants $f(\omega)$ and the Dedekind eta function $\eta(\omega)$ enter theta constants e.g. $\theta(0, \omega) = \eta(\omega) f^2(\omega)$ over which iteration goes. GCR is best modelled by a diffusion equation [24] [25]

$$\left(\frac{\partial}{\partial \tau} - D \sum_l \Delta_l \right) \varphi(x, \tau) = Q(x, \tau) \tag{4}$$

for flux $\varphi(\mathbf{x}, \tau)$ with Dirichlet Laplacian Δ_l and point like sources

$$Q(x, \tau) = \sum_{l=1}^N q_l \delta(x - x_l) \delta(\tau - \tau_l) \tag{5}$$

with diffusion coefficient D . Each γ -step k is a universe or galaxy-like cylindrical segment $dV_t(k) = d^3\mathbf{x} = d(2\pi R^2(t)h)$ with bifurcating toroidal hypersurface $d\sigma_4 = d\tau d^3\mathbf{x} = d\tau dV_t$ of age $\tau = \tau_k$. A complex age τ with complex curvature gets a five-dimensional hypersurface $d\sigma_4 \rightarrow d\sigma_5$. The GCR-flux observed on Earth is ruled experimentally by a probability distribution

$$p(\varphi) = \frac{1}{V_t} \int d\sigma_5 \delta(\varphi - \varphi(x, \tau)) \tag{6}$$

Within FZU charge quanta is traversing definite zeros $\lambda \simeq z_{nt}$ of the Riemann zeta function $\zeta(z)$. Dirac sea symmetry which requires a more drastic revision of fundamental concepts [26] is implicit in FZU. One-dimensional quadratic maps $\gamma(\phi_3(f(\sqrt{\Delta})))$ create cubic binary invariants. Starting from a zero $z_{nt} \simeq \lambda$ rational values of ξ are created. Flux as temperature potential φ in (4) satisfies a one-dimensional heat equation

$$\left(\frac{\partial}{\partial \tau} - \frac{d^2}{du^2} \right) \varphi(u, \omega) = 0 \tag{7}$$

if a four-dimensional equation for mass m exists.

$$\left(\frac{d^2}{du^2} - D\Delta_l \right) \varphi(x, u) = m\varphi(x, u) \tag{8}$$

The Klein-Gordon Equation (8) results from a quadruple of simplest chaotic cycles as a norm $N(f)\zeta(\log f, \mathcal{L})$ with geometric zeta function $\zeta(\log f, \mathcal{L})$ of string \mathcal{L} in FZU [27]. A regularized time

$d\tau \rightarrow (du)^2 \rightarrow \gamma \circ du \rightarrow \gamma \circ \dots \circ \gamma \circ du$ corresponds to a consecutive additive model of creation of matter [8]. A mean free path can vary from zero to ∞ where the diffusion coefficient $D(\tau) = \frac{(dx)^2}{d\tau} \rightarrow D(u) \rightarrow \frac{(dx)^2}{(du)^2} \rightarrow c^2$ changes into the

speed limit for chaotic simplest cycles. Chaotic simplest cycles are equivalent to a tidal interaction of aerosol-liquid-like points $1, 2, 1', 2'$ which is a quadrupolar interaction giving background permeability $\varepsilon_0(\mathbf{k}) = 1/I_{ij} \mathbf{k}_i \mathbf{k}_j$ with moment of inertia I_{ij} and $1/R^3$ behavior [28] [23]. The background susceptibility $\varepsilon_o \simeq R^2$ describes a quadrupolar interaction in E_{exc} . Clouds encapsulate for steps $k \rightarrow \infty$ into a quantum of charge pinned at z_{nt} . An estimation in [24] of φ -dependent

spectral index α in the cumulative flux $C(\varphi) = \int_{\varphi}^{\infty} d\varphi' p(\varphi') \simeq \frac{d\sigma_5}{V_t} \simeq \varphi^{-\alpha}$ can

be circumvented by setting $V_t \simeq 2\pi R^2 h_N \simeq R^2 K^2 \simeq \mathcal{G}_{00}^8$ and

$d\sigma_5 \simeq 2\pi R^2 h_N d\tau \simeq 2\pi R^2(t) h_N \delta_k \omega$ where

$\delta\omega_k = \omega_{k+1} - \omega_k = (\delta_F - 1)(\omega_{k+2} - \omega_{k+1}) \simeq \mathcal{G}_{00} \delta_k \mathcal{G}_{00}$ and $\delta_k \mathcal{G}_{00} = 1$. This gives

$\varphi \approx \mathcal{G}_{00}$ and $\alpha = 3$ in distinction to a high-energy tail of $\alpha = 7/3, 8/3$ where δ_f is the Feigenbaum constant [25]. Equation (7) is solved by the Jacobi theta function $\mathcal{G}(v, \omega)$ on a cylindrical element $dV_i(k)$ of a toroidal bifurcating general Riemann surface \mathbb{C}^5 of cross section with radius $\omega_k \approx \varphi_k = K + iK' \approx R(t) \approx \pi \mathcal{G}_{00}^2$. A quadratic map γ is consistent with modular units $\tau \rightarrow \gamma \circ \tau$, $\omega \rightarrow \gamma \circ \omega$, $u = a\omega \rightarrow a\gamma \circ \omega$ where $a = (r, s)$ is rational which explains a point-like injection term as a new GCR-source k in $Q(x, \tau)$ by period-doubling $\omega_k \rightarrow \omega_{k+1} + \omega_{k+2}$. This chaotic, extensive tree system obeys pseudo-congruent k -components of λ on unit circle in interval $[0, 1]$ for fluctuating coverings $v_k = u/2K^2$ on torus $\mathcal{G}(v, \omega_k) = \mathcal{G}(v+1, \omega_k)$. The chaotic tree with $v = u/2K^2$ is realized by addition on elliptic curves where period-doubling generates new binary invariants which can be expressed by theta constants $\mathcal{G}(a\omega, \omega) \approx \mathcal{G}(0, \omega)$. Up to averaging over a quadruple of steps of a simplest cycle the Dirac current $\bar{\psi} \lambda_m \psi$ is equivalent to the stress-energy tensor in λ and $\lambda' = 1 - \lambda$. Self-similar curvature fluctuations would fill geosphere, biosphere and atmosphere.

4. A Possible Use of BST Energy

For GCR vacuum energy density $\rho_{vac} = 1 \text{ eV} \cdot \text{cm}^{-3}$ atmosphere clouds of volume 10^{15} cm^3 get an energy 10^{15} eV . A geosphere (solid Earth, Earth core) rest mass energy density of $10^0 \text{ g} \cdot \text{cm}^{-3}$ would be 10^{35} times larger. Both spheres are treated uniquely as a fractal FZU set. The ratio of the number of positive air ions to the number of negative air ions is called unipolarity ratio. In vegetation areas an average unipolarity ratio 0.65 is measured which is good for health [11] [12]. Whereas GCR are destructive vegetational negative air ions are beneficial for human and animal [11] [12]. Measured GCR rates of 2 and 20 - 30 ion-pairs $\cdot \text{cm}^{-3} \cdot \text{s}^{-1}$ between ground level and higher atmosphere are detected by large area arrays. Large area correlation is conjectured to be inherent for real spacetime on the basis of complex non-stationary processes. Air ions ρ_{ion} in vegetation are measured locally. The paper conjectures that correlated BST k -components explain QE as well plant correlation and atmospheric clouds up to exosphere [23]. As an experimental confirmation of pseudo-congruence, a global temperature potential V_T is periodic: V_T oscillates between exosphere and Earth's inner core between 1500°C and 5200°C . In [14], cloud formation is related to an alternating RC circuit-like negative differential resistance of atmosphere currents. Simulated altitude variations of GCR counts as well CCN concentrations are on S-shaped negative differential curves. Thus, the altitude vs. GCR flux is an S-shaped negative differential [3] [29]. Volume and energy for open thermodynamic systems cannot be defined. A zero-energy state is e.g. a universe. Its radius R in the Friedmann solution is treated in FZU as an effective potential for drift and diffusion. For vegetational ion density $\rho_{ion} = 10^5 \text{ cm}^{-3}$ the Planck energy M_p is achieved in a volume of 1 km^3 . Lightning bang energy of $1 \text{ GJ} \approx 10^{-5} \text{ g} \approx 0.5 M_p \approx 10^{28} \text{ eV}$ is comparable to the

Planck energy. The energy M_p is localized in small cavities. A GCR density $\rho_{vac} = 1 \text{ eV} \cdot \text{cm}^{-3}$ for a sphere of radius 10^6 m compares to that of the OMG particle. FZU implies invariant curvature and stress-energy as a complex quantity. Curvature as e.g. Bezout matrix $\frac{\varphi(z) - \varphi(w)}{z - w}$ is a constant sum of real and complex spacetime. The amount of dark, non-radiative, non-dissipative matter is a complex cubic functional of the radius. The negative differential curvature-radius-dependence yields a current in a chaotic RC-circuit. Energy would be stored in a BST-component, which is capacitive [14] [28]. The elliptic symmetry $\lambda \rightarrow 1/\lambda$ in (3) suggests that atmospheric and massive components are correlated. Like charge separation by waterfall and aerodynamic breakup two fragments are coupled together with atmospheric showers. This third complex BST-component is viewed as dark matter for zero-energy states. The stored complex energy supplements, e.g., biomass energy. Plant growth simulations support a quadratic map [18] [30]. CRCCS are three-component large and small fragments coupled to a dark, non-radiative, non-dissipative complex spacetime. Lightning bang and thunder fit into FZU as a superfluid with second sound. Weak biophoton emission [31] and measured ionization in vegetational areas seem to be correlated with complex BST states. The question is about the correlation length, which can be large within CRCCS. In the extreme case, an earthward balanced tree of non-ergodic showers (GCR, muons, photons) spreads with the speed of light c with large mean free paths. The claim is that it would be correlated with a slow skyward organic tree [32]. Quasi-ergodic maps would imply atmospheric clouds correlated with radiative forcing to the biosphere. The number of zeros of $\xi(z)$ as zero-energy-states is equivalent to charges in BST. Vegetational air ions would indicate that a third dark (non-radiative, non-dissipative) BST component also exists, as shown in **Figure 2**. Atmospheric ions affect the environment in which photosynthesis occurs, but they don't fundamentally change the way photosynthesis uses light to create energy [20] [33].

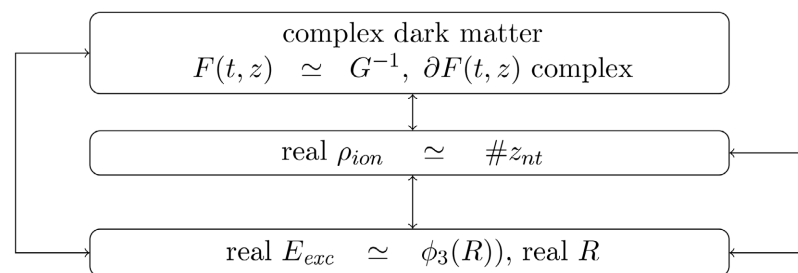


Figure 2. Real and complex correlation within a BST-environment.

As a result, ultra-high particles of low count rate could be emitted. From GCR and CMB with $\rho_{vac} \approx 1 \text{ eV} \cdot \text{cm}^{-3}$ an energy gain can hardly be extracted. Also, harvesting lightning or GCR energy seems hopeless due to short, unexpected pulse rates. CRCCS would imply a controllable dark BST-component next to ionic fragments. It would be capable to store ultra-high energies at plants and at QH. Con-

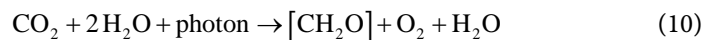
trollable transitions between QH plateaus or equivalently, growing leaves are expected to activate BST [23].

5. Photosynthesis and Correlation

Density and energy for self-similar objects are not uniquely defined and range from zero to infinity. OMG energy (10^{21} eV or Planck energy ($M_p \approx 10^{-5}$ g $\approx 10^{28}$ eV)) is equivalent to heat 12 g water or an atmospheric cloud of 5×10^8 g by 1 K. FZU claims that air ions in vegetation areas arise from stored correlated fractal heat energy as a temperature potential

$$V_{T_{global}} = \int \nabla V_{T_{cloud}} dl_{xy} \tag{9}$$

A potential difference ΔV_T between two points on a straight line may be quite large which is incorporated in quantum statistics (QS) by replacing a fractal segment $dl_{xy} \rightarrow e dl$ by a differential dl with charge coupling e . On a self-similar fractal line element dl_{xy} ΔV_T can become zero. At the same time it is claimed that ΔV_T is capable to develop large correlated energies on differentiable segments. Correlations of ∇V_T are measured by oscillations of global temperature [2]. A chemical reaction between water, carbon dioxide, carbohydrate and oxygen



is set in context to binary invariants. Organic molecules (10) are supposed to be in one-to-one relation to iterated binary invariants $f(\sqrt{\Delta})$ within a controversial discussion of binary invariant theory [34]. In 1900 it was shown that photosynthetic reactions (10) are in one-to-one relation to iterated binary invariants which are also related to $f(\sqrt{\Delta})$. Linear quadratic, cubic and quartic polynomial invariants are symbols h_x, o_x^2, n_x^3, c_x^4 . Tetravalent carbon is $C \approx c_x^4$, oxygen is $O \approx o_x^2$, nitrogen is $N \approx n_x^3$, hydrogen is $H \approx h_x$. The water molecule gets the binary invariant $(oh)^2$ and carbon dioxide gets $(co)^2$. The symbolic invariant $(ab)^2$ is the discriminant of a symbolic quadratic polynomial a_x^2 . Discriminants Δ obey a relation to organic molecules. FZU iterates the Weber invariant $f(\sqrt{\Delta})$ and real algebraic unit $E^{h_\Delta} = \varepsilon \bar{\varepsilon} \rightarrow e^{\det \ln \varepsilon \bar{\varepsilon}} = \frac{1}{2} f^3(\sqrt{\Delta})$ with class number h_Δ , discriminant Δ of elliptic curves and complex conjugated units ε . The symbolic form of a discriminant $(ab)^2$ stands symbolically for the water and carbon dioxide molecule within binary invariant theory. The claim is that photosynthesis starts from discriminants $\Delta \approx 2^8 / f^{48}(\omega)$ which are equivalent to molecules $(oh)^2$ and $(co)^2$ within a correlated quadratic $f(\sqrt{\Delta})$ -map. The existence of a finite number of binary invariants is viewed as a finite number of organic molecule species placed within atmospheric cycles. Iterating (3) $f(\sqrt{\Delta})$ becomes spherical (molecules, atoms) and contains all crystallographic groups for complex γ fixpoints. Starting with an initial point $\xi(z_k)$ fixed

points of the sequence $\gamma(\phi_3(f(\sqrt{\Delta}))) \circ \dots \circ \gamma(\phi_3(f(\sqrt{\Delta}))) \circ x(z_k)$ denote a correlation between discriminants $\Delta = 2^8 / f^{48}(\sqrt{\Delta})$. FZU supports this claim by a charge definition and a relation to quantum statistics. The λ to mass m relation (2) proves that the invariant $f(\sqrt{\Delta})$ relates to masses and charges. Charges and masses would be related to $z_{nt} = \frac{1}{2} + im_n$. The ξ -function $\xi(z \neq z_{nt}) \rightarrow \infty$ in the vicinity of z_{nt} contains a product $\prod_K(z \neq z_{nt})$ like a cloud of infinite mass. Replacing the argument z by the differential operator ∂_z the map $\gamma \circ z$ is conjugate to z^2 which is a Laplace operator Δ_{xy} . The generating function $\xi(z = z_{nt})$ satisfies the Laplace equation. Together with a Lagrange condition $\xi(z_{nt}) = 0$ a two-dimensional Dirichlet problem appears. A quadratic map of the differential operator ∂ yields the Laplacian. A fractal string $z = f(\sqrt{\Delta})$ in the geometric zeta function $\zeta(z, \mathcal{L})$ replaced by the differential operator ∂ corresponds to $\Delta_{xy}\xi(z) + \mu\xi(z)$. Charge defining zeros are partial solutions of a Dirichlet Laplacian as periodic solutions related to [27]. Invariant theoretic results get relevant to quantum mechanics for a scanning cubic field of $f(\sqrt{\Delta})$ [23].

The quadratic map $\gamma(\phi_3(f(\sqrt{\Delta}))) \circ z = F(t, z)$ is a rational Hermite-Tschirnhausen map $F(t, z)$ which envelopes QS. The function $F(t, z)$ is equivalent to an inverse Green's function [35]. A bi spinor is a quadruple of steps k with invariant B_8 . This is equivalent to one addition step on an elliptic curve enveloped by hyperelliptic parametrizations. Subsequent $F(t, z)$ create the set of finitely generated binary invariants [35]. The linear map $\gamma(\phi_3(f(\sqrt{\Delta})))$ can be set in context to QS and to the property of spin. In FZU the Legendre module λ is viewed as a current density. Together with its involution $i(l)$ the current density depends on binary invariants $f(\sqrt{\Delta})$. It is claimed that the BST-state of involution (3) correlates large and small matter fragment. Atmosphere and geosphere and Earthward and skyward non-ergodic flows are claimed to be correlated by (3). In FZU k step-pseudo-congruence is expected if the dimensionless dark matter coupling constant G_5 equals the k-component at $G_5^{-1} = 2^{2^k}$. Values $k = 9, 10$ explain that QS overestimates ρ_{vac} by hundreds of orders of magnitude (CCP) [13] [23]. The agreement of QS with experiment is explainable by the $\rho_{core} - \rho_{vac}$ symmetry in Equation (3).

6. Conclusion

A cloud radiative forcing hypothesis (GCR-CN-CCN) is extended to biosphere and to photosynthesis. A model of continuous creation of matter corresponds to a complex Lagrangian. With low count rate of real processes, it contains complex dark scattering. It is claimed that the complex Lagrangian is not exotic but is a

stationary state as a source of real spacetime. FZU explains cosmological redshift and cosmic rays by quadrupolar processes. Photosynthesis is possibly bound to GCR-BST-sources, explaining measured high values of ρ_{ion} in vegetation areas as well as measured biophotons [14] [31]. Besides, biomass energy harvesting dark matter energy from the complex component would be like harvesting lightning energy. However, the analogy to QH would offer controlled ion separation by external fields. Highly correlated k-components from geosphere, biosphere, to atmosphere would explain QE in daily life. Mathematically, clouds and charges are linked to nontrivial zeros z_n of zeta functions [13]. A quadrupolar configuration of four conjugated zeros z_n describes a nearly neutral zero-energy state. This quadratic-in-mass equation is like a tidal self-interaction having negative and complex solutions as phantom energies in van der Waals forces.

Acknowledgements

Sincere thanks to reviewers of JMP and SCIRP for critical, valuable comments in encouraging the presented unified approach.

Conflicts of Interest

The author declares no conflicts of interest regarding the publication of this paper.

References

- [1] Svensmark, H. (1998) Influence of Cosmic Rays on Earth's Climate. *Physical Review Letters*, **81**, 5027-5030. <https://doi.org/10.1103/physrevlett.81.5027>
- [2] Svensmark, H., Svensmark, J., Enghoff, M.B. and Shaviv, N.J. (2021) Atmospheric Ionization and Cloud Radiative Forcing. *Scientific Reports*, **11**, Article No. 19668. <https://doi.org/10.1038/s41598-021-99033-1>
- [3] Yu, F. (2001) Cosmic Rays, Particle Formation, Natural Variability of Global Cloudiness, and Climate Implications. <https://cds.cern.ch/record/557174/files/p101.pdf>
- [4] Yu, F., Turco, R.P. and Kärcher, B. (1999) The Possible Role of Organics in the Formation and Evolution of Ultrafine Aircraft Particles. *Journal of Geophysical Research: Atmospheres*, **104**, 4079-4087. <https://doi.org/10.1029/1998jd200062>
- [5] Matsumoto, H. (2022) Cosmic Rays and Aerosols in Earth's Atmosphere and Their Role in Cloud Formation. Ph.D. Thesis, Technical University of Denmark.
- [6] Ziep, O. (2024) Nucleosynthesis in Thin Layers. <https://www.epubli.de>
- [7] Ziep, O. (2024) Fractal Zeta Universe and Cosmic-Ray-Charge-Cloud Superfluid, www.epubli.de, Berlin. <https://doi.org/10.5281/zenodo.14193126>
- [8] Dirac, P.A.M. (1974) Cosmological Models and the Large Numbers Hypothesis. *Proceedings of the Royal Society A: Mathematical, Physical and Engineering Sciences*, **338**, 439-446. <https://doi.org/10.1098/rspa.1974.0095>
- [9] Amerongen, H.v., Grondelle, R.v. and Valkunas, L. (2000) Photosynthetic Excitons. World Scientific Publishing Co. Pte. Ltd. <https://doi.org/10.1142/9789812813664>
- [10] Kassel, L.S. (1930) The Binding Energy of Some Organic Compounds. *Nature*, **125**, 926-926. <https://doi.org/10.1038/125926a0>
- [11] Patil, G.B., Pawar, S.D., Bhosale, J.L. and Patil, P.G. (2021) Pollution Index and Air Ion Variation in Different Vegetation Area at the Rural Station Bhilawadi (16°59'n,

- 74° 28'e). *Journal of Physics: Conference Series*, **1964**, Article ID: 032006. <https://doi.org/10.1088/1742-6596/1964/3/032006>
- [12] Pawar, S.D., et al. (2023) Air Quality and Air Ion Assessment Ratio for Papaya, Chickpea, and Guava Vegetation Area at Rural Station Khatavs (16 o 57'N, 74 o 31'E). https://www.researchgate.net/publication/375005153_Air_Quality_and_Air_Ion_Assessment_Ratio_for_Papaya_Chickpea_and_Guava_Vegetation_Area_at_Rural_Station_Khatav_16_o_57'N_74_o_31'E
- [13] Ziep, O. (2025) Charge Quanta as Zeros of the Zeta Function in Bifurcated Spacetime. *Journal of Modern Physics*, **16**, 249-262. <https://doi.org/10.4236/jmp.2025.162011>
- [14] Ziep, O. (2025) Fractal Universe and Atoms. *Scholars Journal of Physics, Mathematics and Statistics*, **12**, 89-96. <https://doi.org/10.36347/sjpm.2025.v12i04.002>
- [15] Kolarz, P., Gaisberger, M., Madl, P., Hofmann, W., Ritter, M. and Hartl, A. (2012) Characterization of Ions at Alpine Waterfalls. *Atmospheric Chemistry and Physics*, **12**, 3687-3697. <https://doi.org/10.5194/acpd-11-25297-2011>
- [16] Zilch, L.W., Maze, J.T., Smith, J.W., Ewing, G.E. and Jarrold, M.F. (2008) Charge Separation in the Aerodynamic Breakup of Micrometer-Sized Water Droplets. *The Journal of Physical Chemistry A*, **112**, 13352-13363. <https://doi.org/10.1021/jp806995h>
- [17] Wu, R. (2017) Research on Generation of Negative Air Ions by Plants and Stomatal Characteristics under Pulsed Electrical Field Stimulation. *International Journal of Agriculture and Biology*, **19**, 1235-1245. <https://doi.org/10.17957/ijab/15.0431>
- [18] Arora, V.K. and Boer, G.J. (2006) Simulating Competition and Coexistence between Plant Functional Types in a Dynamic Vegetation Model. *Earth Interactions*, **10**, 1-30. <https://doi.org/10.1175/ei170.1>
- [19] Heegner, K. (1952) Diophantische Analysis und Modulfunktionen. *Mathematische Zeitschrift*, **56**, 227-253. <https://doi.org/10.1007/bf01174749>
- [20] Ziep, O. (2025) Metric Stability and Jacobi-Gauss Periods. <https://doi.org/10.5281/zenodo.16895381>
- [21] Jacobi, C.G.J. (1846) Über die Kreistheilung und ihre Anwendung auf die Zahlentheorie. *Journal für die reine und angewandte Mathematik*, **33**, 166-182.
- [22] Friedmann, A. (1922). On the Curvature of Space. *Zeitschrift für Physik*, **10**, 377.
- [23] Ziep, O. (2025) Matter and Quantum Entanglement. *Journal of Applied Mathematics and Physics*, **13**, 1125-1137. <https://doi.org/10.4236/jamp.2025.134059>
- [24] Genolini, Y., Salati, P., Serpico, P.D. and Taillet, R. (2017) Stable Laws and Cosmic Ray Physics. *Astronomy & Astrophysics*, **600**, A68. <https://doi.org/10.1051/0004-6361/201629903>
- [25] Bernard, G., Delahaye, T., Salati, P. and Taillet, R. (2012) Variance of the Galactic Nuclei Cosmic Ray Flux. *Astronomy & Astrophysics*, **544**, A92. <https://doi.org/10.1051/0004-6361/201219502>
- [26] Dirac, P.A.M. (1931) Quantised Singularities in the Electromagnetic Field. *Proceedings of the Royal Society A: Mathematical, Physical and Engineering Sciences*, **133**, 60-72.
- [27] Herichi, H. and Lapidus, M.L. (2012) Riemann Zeros and Phase Transitions via the Spectral Operator on Fractal Strings. *Journal of Physics A: Mathematical and Theoretical*, **45**, Article ID: 374005. <https://doi.org/10.1088/1751-8113/45/37/374005>
- [28] Ziep, O. (2025) A Quantum Entangled Fractal Superfluid Universe. *Journal of High Energy Physics, Gravitation and Cosmology*, **11**, 850-868. <https://doi.org/10.4236/jhepgc.2025.113054>

- [29] McIntosh, G. (2017) Cosmic Ray Air Shower Lateral Coincidence. 2016 *Academic High Altitude Conference*, 29 June-1 July 2016, St. Catherine, 1-6.
<https://doi.org/10.31274/ahac.5565>
- [30] Kupolusi, J.A., Adedeji and Odunayo, S. (2025) Modelling of Aerial Biomass and Its Physicochemical Properties Using Artificial Intelligence and Response Surface Methodology. *Scholars Journal of Physics, Mathematics and Statistics*, **12**, 33-42.
<https://doi.org/10.36347/sjpms.2025.v12i03.001>
- [31] Salari, V., Seshan, V., Frankle, L., England, D., Simon, C. and Oblak, D. (2024) Imaging Ultraweak Photon Emission from Living and Dead Mice and from Plants Under Stress. *The Journal of Physical Chemistry Letters*, **16**, 4354-4362.
- [32] Tanaka, H.K.M. (2025) Distance of Flight of Cosmic-Ray Muons to Study Dynamics of the Upper Muosphere. *Geoscientific Instrumentation, Methods and Data Systems*, **14**, 1-11. <https://doi.org/10.5194/gi-14-1-2025>
- [33] Timpmann, K., Rätsep, M. and Freiberg, A. (2023) Enhancing Solar Spectrum Utilization in Photosynthesis: Exploring Exciton and Site Energy Shifts as Key Mechanisms. *Scientific Reports*, **13**, Article No. 22299.
<https://doi.org/10.1038/s41598-023-49729-3>
- [34] Gordan, P. and Alexejeff, W. (1900) Übereinstimmung der Formeln der Chemie und der Invariantentheorie. *Zeitschrift für Physikalische Chemie*, **35**, 610-633.
<https://doi.org/10.1515/zpch-1900-0141>
- [35] Ziep, O. (2025) Topological Entropy of Regular Chaotic Quadratic Maps. *Scholars Journal of Physics, Mathematics and Statistics*, **12**, 43-58.
<https://doi.org/10.36347/sjpms.2025.v12i03.002>